frontiers in Endocrinology

ORIGINAL RESEARCH
published: 24 May 2019
doi: 10.3389/fendo.2019.00307

Evolutionary Conservation of Thyroid Hormone Receptor and Deiodinase Expression Dynamics *in ovo* in a Direct-Developing Frog, *Eleutherodactylus coqui*

Mara Laslo[1]*, *Robert J. Denver*[2] *and James Hanken*[1]

[1] *Department of Organismic and Evolutionary Biology, and Museum of Comparative Zoology, Harvard University, Cambridge, MA, United States,* [2] *Departments of Molecular, Cellular and Developmental Biology, and Ecology and Evolutionary Biology, University of Michigan, Ann Arbor, MI, United States*

OPEN ACCESS

Edited by:
Marco António Campinho, Center of Marine Sciences (CCMAR), Portugal

Reviewed by:
Paula Duarte-Guterman, University of British Columbia, Canada
Salvatore Benvenga, University of Messina, Italy

***Correspondence:**
Mara Laslo
mlaslo@g.harvard.edu

Specialty section:
This article was submitted to Thyroid Endocrinology, a section of the journal Frontiers in Endocrinology

Received: *05 February 2019*
Accepted: *29 April 2019*
Published: *24 May 2019*

Citation:
Laslo M, Denver RJ and Hanken J (2019) Evolutionary Conservation of Thyroid Hormone Receptor and Deiodinase Expression Dynamics in ovo in a Direct-Developing Frog, Eleutherodactylus coqui. Front. Endocrinol. 10:307. doi: 10.3389/fendo.2019.00307

Direct development is a reproductive mode in amphibians that has evolved independently from the ancestral biphasic life history in at least a dozen anuran lineages. Most direct-developing frogs, including the Puerto Rican coquí, *Eleutherodactylus coqui*, lack a free-living aquatic larva and instead hatch from terrestrial eggs as miniature adults. Their embryonic development includes the transient formation of many larval-specific features and the formation of adult-specific features that typically form postembryonically—during metamorphosis—in indirect-developing frogs. We found that pre-hatching developmental patterns of thyroid hormone receptors alpha (*thra*) and beta (*thrb*) and deiodinases type II (*dio2*) and type III (*dio3*) mRNAs in *E. coqui* limb and tail are conserved relative to those seen during metamorphosis in indirect-developing frogs. Additionally, *thra, thrb,* and *dio2* mRNAs are expressed in the limb before formation of the embryonic thyroid gland. Liquid-chromatography mass-spectrometry revealed that maternally derived thyroid hormone is present throughout early embryogenesis, including stages of digit formation that occur prior to the increase in embryonically produced thyroid hormone. *Eleutherodactylus coqui* embryos take up much less 3,5,3′-triiodothyronine (T_3) from the environment compared with *X. tropicalis* tadpoles. However, *E. coqui* tissue explants mount robust and direct gene expression responses to exogenous T_3 similar to those seen in metamorphosing species. The presence of key components of the thyroid axis in the limb and the ability of limb tissue to respond to T_3 suggest that thyroid hormone-mediated limb development may begin prior to thyroid gland formation. Thyroid hormone-dependent limb development and tail resorption characteristic of metamorphosis in indirect-developing anurans are evolutionarily conserved, but they occur instead *in ovo* in *E. coqui*.

Keywords: embryo, direct development, thyroid hormone, amphibians, evolution, metamorphosis, maternal effects, life history

INTRODUCTION

Direct development, a distinctive life-history mode in amphibians and other animals, has evolved in anurans multiple times from the ancestral biphasic life history; it characterizes many hundreds of living species (1). Even though direct-developing frogs typically lack both a free-living aquatic larval stage and a discrete, post-hatching metamorphosis, many species display a cryptic metamorphosis before hatching: adult-specific features, such as limbs, form precociously in the egg, and numerous tadpole-specific features are present initially but then are lost [**Figure 1**; (2, 3)]. Because such changes in frogs with indirect development are mediated by thyroid hormone (TH), the primary regulator of metamorphosis (4), evolutionary change in thyroid axis function and timing may underlie the numerous heterochronies observed between direct-developing and indirect-developing species (5–9). Yet, there have been few attempts to precisely delineate the role of this or other pertinent physiological mechanisms.

Embryonic development of direct-developing frogs, as seen in the Puerto Rican coquí, *Eleutherodactylus coqui*, appears to comprise a mosaic of TH-independent and TH-dependent features. We use the term "embryonic" to describe all *in ovo* development in *E. coqui*, although this period encompasses both the initial formation of major organ systems as well as the patterning, morphogenesis and growth that follows. Many of the latter events correspond to metamorphic changes in biphasic anurans. It was once thought that embryonic development in direct-developing species was primarily TH-independent (5). However, subsequent studies with exogenous T_3 and with TH-synthesis inhibitors suggested at least a partial role for TH in terminal stages of limb development as well as tail resorption (6, 10). In *E. coqui*, for example, treatment with exogenous T_3 causes precocious tail resorption but has little to no effect on limb elongation (11). Similarly, treatment with methimazole, a TH-synthesis inhibitor, inhibits only tail resorption and late stages of limb elongation but does not affect early limb differentiation or digit formation (8). The apparent TH-independence of early stages of limb development is correlated with the fact that limb bud, paddle and digit formation occur prior to formation of the embryonic thyroid gland [**Figure 1**; (12, 13)]. Thus, limb development in *E. coqui* comprises two periods: limb bud differentiation and paddle and digit morphogenesis, which precede formation of the thyroid gland and may be TH independent; and limb growth and elongation, which follow thyroid gland formation and are TH dependent. Experiments with TH-synthesis inhibitors, however, can only address the role of TH in the second period. The presumed TH independence of the first period remains to be verified experimentally.

All organs in the body are exposed to roughly the same concentration of circulating TH, primarily in the form of thyroxine (T_4) and lower concentrations of 3,5,3′-triiodothyronine [T_3; (14, 15)]. Hereafter, we use the term TH to refer to both T_4 and T_3. However, tissue-specific differences in uptake, metabolism, and action provide for diverse effects of TH in different tissues. Thus, tissue-specific changes in TH metabolism and action likely contribute to the heterochrony of developmental events observed in direct-developing anurans relative to biphasic species. Alternatively, the principal locus of change in hormonal control may involve a shift in the source of THs and when they are present in the embryo. Maternally derived TH is present at early developmental stages of all vertebrates examined so far. In most vertebrates, maternal TH is in the yolk; in most mammals, maternal TH can pass from mother to fetus via the placenta or milk. Yet, the role of maternally derived TH in amphibian embryos is poorly understood (16–18). If maternally derived THs are present in early embryos of *E. coqui*, they could influence limb development prior to formation of the embryonic thyroid gland. Finally, three different deiodinase enzymes control cellular metabolism of T_4 in target tissues. In amphibians, two types of deiodinases play major roles during development. Deiodinase enzyme type II (Dio2) converts T_4 into T_3, which has at least 10 times greater affinity for TH receptors (TRs) than T_4. Deiodinase type III (dio3) converts T_4 to both T_2 and reverse triiodothyronine (rT_3), which are unable to bind TRs in most species. Thyroid hormones act by binding to two TR subtypes, designated alpha (α) and beta (β), to activate or repress transcription of TH target genes. Contrasting expression patterns of TRs and deiodinases may in part underlie the diverse, tissue-specific effects of TH in *Xenopus* species (19–26), and it is likely that changes in the temporal or spatial expression of deiodinases or TRs influence TH competence and action in target tissues in *E. coqui*.

Here we tested the hypothesis that developmental changes in TR and deiodinase mRNAs in developing *E. coqui* limb and tail, and in whole body TH content are conserved relative to those seen during metamorphosis in indirect-developing frogs. We also investigated whether *E. coqui* tissues are capable of responding directly to T_3 action by mounting gene regulation responses similar to those seen in metamorphosing species. Taken together, our data support the hypothesis that limb development and tail resorption in *E. coqui* (8, 12) are mediated by conserved components of TH signaling. Additionally, our results suggest that maternal TH could facilitate limb development prior to formation of the embryonic thyroid gland.

MATERIALS AND METHODS

Animal Care

Live adult *Eleutherodactylus coqui* were field-collected from introduced populations in Hilo, Hawaii, with the permission of the U.S. Fish and Wildlife Service (permits EX-14-06, EX-16-07, and EX-17-11). They were brought to Harvard University and maintained as a breeding colony in the Hanken laboratory (IACUC protocol #99-09-03); embryos were obtained following spontaneous matings. Following removal of the overlying chorion with watchmaker forceps in 2% cysteine (pH 8.5) in 10% Holtfreter solution, embryos were reared in 10% Holtfreter solution in Petri dishes at 22.5°C. Embryos were staged according to the normal table of Townsend & Stewart (TS; 1985), which defines 15 stages from fertilization (1) to hatching (15). Following internal fertilization, the adult female deposits embryos at TS stage 1.

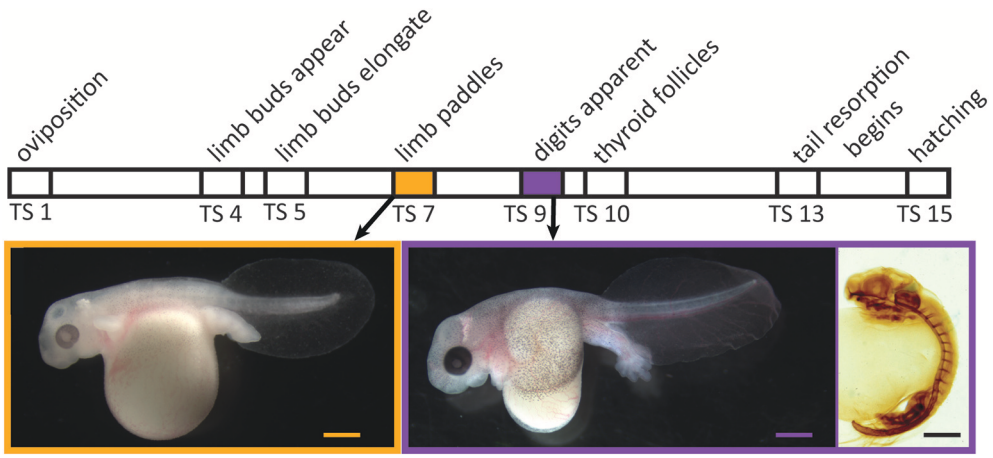

FIGURE 1 | Relative timing of several developmental events during embryogenesis in *Eleutherodactylus coqui*. Images depict live TS stage 7 **(Left)** and stage 9 **(Middle)** embryos removed from overlying egg membranes, and a TS stage 9 embryo **(Right)** stained for type II collagen, which reveals the cartilaginous skeleton and notochord. Scale bars, 1 mm.

Molecular Cloning and Sequence Validation

Partial cDNAs for *dio2*, *dio3*, *thra*, *thrb*, *ribosomal protein L8* (*rpL8*), *thyroid hormone induced bZip protein* (*thibz*), and *alpha-actinin 4* (*actn4*) (Genbank accession numbers MK784754, MK784753, MK784748, MK784749, MK784751, MK784750, MK784755) were isolated by PCR with exact primers (**Table 1**) using cDNA generated from RNA isolated from whole TS stage 13 embryos, and the resultant DNA fragments were subcloned into the pCR II plasmid. Exact primers for *dio2*, *dio3*, *thra*, *thrb*, *rpL8*, and *thibz* were designed from predicted full-length cDNA sequences provided by L. Sachs, N. Buisine, and G. Kerdivel (personal communication), while *actn4* primers were designed from genomic sequences provided by A. Mudd, R. Harland, and D. Roksahr (personal communication). We also subcloned a partial cDNA for *krüppel-like factor 9* (*klf9*) by degenerate PCR (oligonucleotide primers designed using CODEhop) using the same cDNA described above (Genbank accession number MK784752). The sequences of the subcloned partial cDNA fragments were confirmed by direct DNA sequencing and by comparing them against the full-length cDNAs provided by the investigators listed above.

Prior to the full-length predicted cDNA sequences becoming available, oligonucleotide primers for SYBR-based reverse transcriptase quantitative PCR (RTqPCR) were designed based on the available mRNA sequences on Genbank for *thra* and *thrb,* and the previously cloned *rpL8* [Genbank accession numbers AF201957.1 and AF201958.1; (8), **Table 1**]. For probe-based quantitative PCR (qPCR), primers and probes for *actn4* were designed from the partial cloned cDNA sequence while *dio2*, *dio3*, *thra*, *thrb*, *rpL8*, *thibz*, and *klf9* were designed based on the full-length sequences from other investigators listed above (Genbank accession numbers MK784763, MK784762, MK784757, MK784756, MK784760, MK784758, MK784759, MK784761).

Whole Body Extraction and Quantification of Iodothyronines Using LC-MS/MS

The iodothyronines T_3, rT_3, T_4, and T_2 were quantified from whole *E. coqui* embryos throughout development. Because embryos were not dissected from the yolk, all measurements include embryo and yolk TH content. Animals at different stages were anesthetized and snap frozen until extraction and LC-MS/MS analysis. Unfertilized oocytes were dissected from the ovaries of a newly sacrificed female and snap frozen. Between 15 and 20 embryos (∼ 600 mg) were pooled to make one biological replicate. Three or four biological replicates were used for each developmental stage. Tissues were extracted for thyroid hormone analysis as described by Denver (27, 28) with the following modifications: stable isotope-labeled T_3 and T_4 ($^{13}C_6$ T_3 and T_4, Sigma) were used as an internal standard to correct for differences in extraction efficiency, and solid phase extraction with a Supel-Select SCX cartridge (60 mg 3 mL, Sigma) was used to further purify the extracted tissue. After conditioning the cartridge with 3 mL methanol (HPLC Grade, Sigma) and equilibrating it with 5 mL of 2% formic acid in water (HPLC Grade, Sigma), the sample was loaded, rinsed first with 3 mL 2% formic acid in water and then with 3 mL methanol, and finally eluted with 2 mL of freshly prepared 5% ammonium hydroxide in methanol. It was then evaporated to dryness under nitrogen flow and resuspended in 100 µl of 0.1% formic acid in methanol. Samples were measured at the Harvard Small Molecule Mass Spectrometry facility by using gradient liquid-chromatography mass-spectrometry (LC-MS/MS). Ten microliters of samples were injected on a C18 column (Kinetex 2.6 µm, 100 Å pore size, 150 × 2.1 mm, Phenomenex) in an Agilent 1290 HPLC coupled with an Agilent 6460 Triple Quad Mass Spectrometer. See **Supplementary Information** for the LC and MS parameters (**Supplementary Tables 1, 2**). Calibration curves were made in 0.1% formic acid in methanol with pure standards and the same amount of internal standard as the samples. Quantification

TABLE 1 | Degenerate PCR, exact PCR, and qPCR primers and probes for *Eleutherodactylus coqui* and *Xenopus tropicalis*.

Gene	Type	Species		Sequence	Probe sequence	Amplicon size (bp)
thibz	qPCR	*E. coqui*	F	GAGGGTCAAACGCCAGTATT	TGAAGGGTGCTATAAAGTAGCTGAT	72
			R	GTCCGGGTCTGTGTAATGTC		
klf9	qPCR	*E. coqui*	F	CAAGTCCTCCCACCTCAAAG	CCCACTACAGAGTGCATACAGGTGA	65
			R	CATGTGCATGGAAATGGACG		
rpL8	qPCR	*E. coqui*	F	CTGGAGGTGGACGTATTGAC	ACCCATTCTGAAGGCAGGTCGT	68
			R	TCTTGGCCTTGTACTTGTGG		
dio2	qPCR	*E. coqui*	F	ACACAGTTACCTCAACAGGG	TGCAATCTGATCTCCCAGGAGCA	87
			R	AACAGTGTGGAACATGCAGA		
dio3	qPCR	*E. coqui*	F	GCAGCCCAGCAGTATTATCA	CGTGGAGGACATGCGTTTAACCC	95
			R	CACATGGGTGGTCTCGTTTA		
thra	qPCR	*E. coqui*	F	ACTACATCAACCACCGCAAA	CCCACTTCTGGCCTAAGCTCCT	81
			R	CAATCATGCGCAAGTCAGTC		
thrb	qPCR	*E. coqui*	F	GCAGCCCAGCAGTATTATCA	TCAAATGTTGTGCCTGCGGCT	95
			R	GTGATCACCATGGGAGATGG		
actn4	qPCR	*E. coqui*	F	AAGCCATCTCTGAAGTCCTC	AGTGCCAGCCTTCCTCAGGTG	80
			R	TTTCACGGCTTGGTGTAACT		
rpL8	qPCR	*E. coqui*	F	GACCAGAGTAAAGCTGCCTTCT	SYBR	95
			R	TTGTCAATACGTCCACCTCCAG		
thra	qPCR	*E. coqui*	F	CGACAAAATCACCCGAAATCAGT	SYBR	78
			R	GACAAGGTCCATTGCCATGC		
thrb	qPCR	*E. coqui*	F	CTTGCGCCTCTTTTCTCTGTTT	SYBR	76
			R	CAGATCTGGTTTTGGATGACAGC		
klf9	Degenerate	*E. coqui*	F	GGSTGTGGCAAAGTYTAYGGSAA		215
			R	TTGGTYAARTGRTCRCTCCTCAT		
rpL8	Exact	*E. coqui*	F	GACATTATCCATGATCCAGGCCG		616
			R	CAGTCTTTGTACCGCGCAGACG		
dio2	Exact	*E. coqui*	F	GAGTGTGGACCTGTTGATCACT		745
			R	TTTCTGTTCCATCCACTGTCGT		
dio3	Exact	*E. coqui*	F	TGCAAACTTCTCAAACAGGTGG		716
			R	TTCCTCAGTTCAGCGATCTTGT		
thra	Exact	*E. coqui*	F	AGAGCCAGATGAAAAGAGGTGG		801
			R	CTGTCAGGATCGTAACGCACA		
thrb	Exact	*E. coqui*	F	CTAGCAGCATGTCAGGGTACAT		779
			R	TACCACCCCTAGTCCTCCATTT		
actn4	Exact	*E. coqui*	F	GAAACAGCAGCGGAAGACTTTC		619
			R	CTTCTTATCAGGACGAGCGGTG		
thibz	Exact	*E. coqui*	F	CTCCATGATTCAACTCCACCCA		961
			R	CGTAGTGAGGGTGAGACAACAA		
thibz	qPCR	*X. tropicalis*	F	AAGAGACGCAAGAACAACGA	AGAAGCGCCGGGCGGGGGA	111
			R	GAGTCGGGCATTCTCTTCAA		
klf9	qPCR	*X. tropicalis*	F	AGTCTTCCCACCTTAAAGCC	ACGCCCTTTTCCGTGTACGTGGCCT	106
			R	GTCAACTCATCGGAACGAGA		
eef1a1	qPCR	*X. tropicalis*	F	CTTGACTGCATTTTGCCACC	AGCCTCTGCGTCTGCCTCTGCAGG	112
			R	GTCTCCACACGACCAACTG		
dio3	qPCR	*X. tropicalis*	F	CGGTGCCTACTTTGAGAGAC	TACCAGGGAGGGCGGGGGCC	94
			R	CCGAGATCTTGTAGCCTTCC		
thrb	qPCR	*X. tropicalis*	F	TTGATGATACCGAAGTCGCC	TCGCCCTGGCCTCACTAGTGTGGAGA	102
			R	AACCTTCCTGGCACTTTTCT		
actn1	qPCR	*X. tropicalis*	F	CAAAGTGCTGGCTGTCAATC	AGCTGGCCAGTGATCTGCTGGAGTGG	105
			R	TCTAACCAAGGGATTGTGCG		

results with a signal-to-noise (S/N) ratio >10 were used for the statistical analysis. Results with a ratio between 3 and 10 (purple type; **Supplementary Table 3**) were included in the graph (**Figure 2**) but not used in the statistical analysis; those with a ratio below 3 were not used (red type; **Supplementary Table 3**). We normalized iodothyronine content to the weight of the tissue extracted.

Quantitative PCR

Dechorionated embryos were anesthetized by immersion in 10% Holtfreter solution with drops of 2% neutral-buffered MS-222 added until the embryos no longer responded to toe pinches (between 30 and 60 s). Limbs and tails were dissected and homogenized in TriZol reagent (Invitrogen) and kept at −20°C until RNA isolation. Total RNA was isolated following the manufacturer's protocol within 3 weeks of homogenization. Because qPCR primers did not span exon-exon boundaries, genomic DNA was removed with an Ambion DNA-*free* kit (cat. #AM1906). Controls with no reverse-transcriptase verified that removal of genomic DNA was complete. Total RNA was quantified with a Qubit Fluorometer 3.0 and checked for purity on a Nanodrop spectrophotometer. For SYBR Green RTqPCR assays, 200 ng of total RNA was used for input for each reaction. For probe-based qPCR, 660 ng of total RNA for each sample was synthesized into cDNA with iScript Reverse Transcriptase Supermix for RT-qPCR (BioRad). Complementary DNA was kept at −20°C until the qPCR assay was performed. mRNA levels were analyzed with either Ssoadvanced Universal Probes Supermix (BioRad) or an iTaq Universal SYBR Green One-Step kit (BioRad) on a CFX384 machine. See **Supplementary Data** for qPCR cycling conditions. Optimal qPCR conditions were determined with temperature gradient and cDNA dilutions for dynamic range of input. Standard curves showed high efficiency of reaction (90–105%), and R^2 was equal to or >0.98 for all primer sets. No template controls showed no amplification. All oligonucleotides are listed in **Table 1**. All SYBR and probe-based qPCR experiments were done in simplex. The relative mRNA levels were determined as described by Schmittgen and Livak (29). For the developmental expression studies, target-gene expression was normalized to the reference gene *rpL8*, which did not show significant variation across development [*rpL8* mRNA values are given in **Supplementary Table 5**; see also (8)]. In the *in vivo* and the tissue explant T_3 response experiments, *E. coqui* target gene mRNA levels were normalized to the reference genes *rpL8* and *actn4*, which was unaffected by T_3 treatment. Small, statistically insignificant changes in reference gene mRNAs could have led to a small underestimation of the effect of T_3 in these experiments.

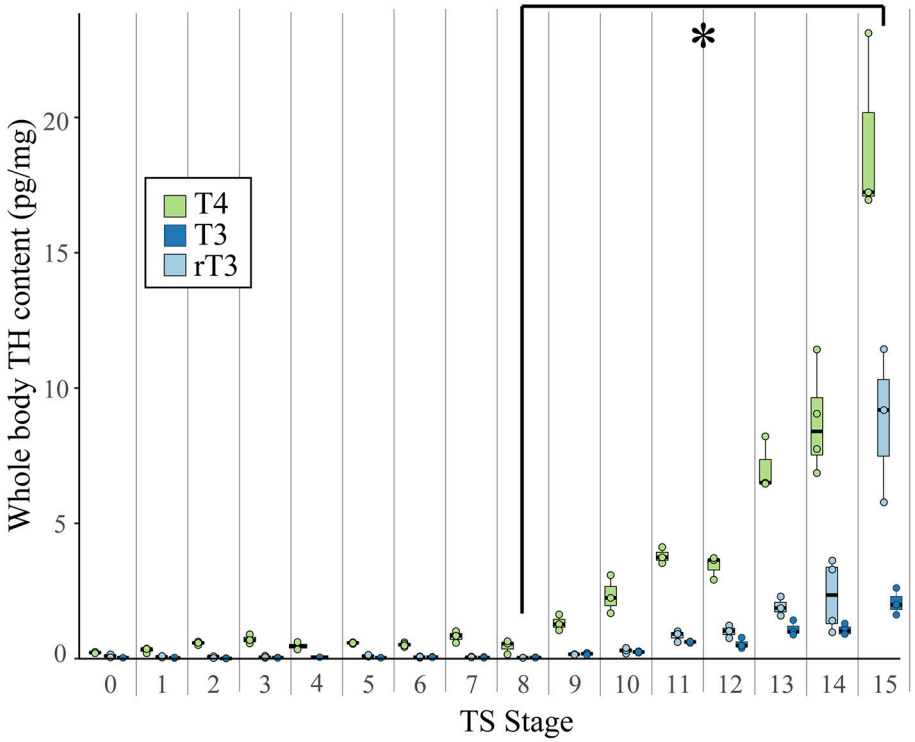

FIGURE 2 | Whole body content of T_4, T_3, and rT_3 in pooled *E. coqui* embryos at TS stages 1–15 and in unfertilized oocytes (TS 0) as quantified by LC-MS/MS. Whole body content of iodothyronines was normalized to sample weight; between 15 and 20 embryos were pooled to generate one biological replicate. Each value depicted in the graph is based on two-to-four replicates. Values based on fewer than three replicates are not included in the statistical analysis. All three iodothyronines increased significantly between TS stages 8 and 15 (*post-hoc* Dunn's test; $p < 0.05$), indicated by the asterisk (*). See **Supplementary Data** for a complete list of significant pairwise differences. Each boxplot represents median and range of the data.

For *Xenopus tropicalis*, qPCR primers and probes for *thrb*, *klf9*, *thibz*, *dio3*, *elongation factor 1 alpha* (*eef1a1*) and *alpha-actinin 1* (*actn1*) were designed from publicly available sequences (Genbank accession numbers XM_012964865.2, NM_001113674.1, XM_018092557.1, NM_001113667.2, NM_001016692.2, and NM_001079198.1). For tissue explant experiments, *X. tropicalis* target gene expression was normalized to *eef1a1* and *actn1*.

Treatment of *E. coqui in vivo*

Eleutherodactylus coqui embryos were dechorionated into 10% Holtfreter solution at least 24 h prior to immersion in T_3. One mM stock T_3 in DMSO or 0.01 N NaOH was diluted to make 50 nM T_3 in 10% Holtfreter solution. We chose 50 nM T_3 because it has been shown to induce tail resorption in *E. coqui* (8), and a 46-h timepoint to allow enough time for induction of T_3 response genes. We chose TS stage 9 embryos because the last third of limb development is TH-dependent (8), but TS stage 9 is still prior to thyroid gland activation. T_3 treatment solutions were refreshed every 8–12 h. After 46 h (n = 12–14 TS-9 embryos), dechorionated embryos were anesthetized as described above and limbs and tails were dissected, from which total RNA was extracted using TriZol reagent.

Measurement of Environmental T_3 Uptake in *X. tropicalis* and *E. coqui*

To determine if *E. coqui* embryos are capable of taking up TH from their surrounding environment, we immersed dechorionated TS stage 9 *E. coqui* embryos or NF 51–55 *X. tropicalis* tadpoles in 30 mL (*E. coqui*) or at least 500 mL (*X. tropicalis*) 10% Holtfreter solution with either 1 nM (n = 4–6 biological replicates/treatment) or 50 nM (n = 3–4 biological replicates/treatment) stable isotope-labeled T_3. We chose TS stage 9 *E. coqui* embryos to match the *in vivo* T_3 treatment experiments and selected *X. tropicalis* tadpoles with developing limbs with similar morphology to *E. coqui* TS stage 9. Approximately twenty *E. coqui* individuals (600 mg tissue) or two tadpoles were pooled were pooled to make one biological replicate. Tadpoles were either ordered from Xenopus1 (Ann Arbor, Michigan, U.S.A.) or derived from the Hanken lab colony. Stock 100 μg/mL stable isotope-labeled T_3 was diluted to either 1 or 50 nM T_3. After either 8 or 24 h in 1 nM labeled T_3 solution or 46 h in 50 nM T_3 solution, *X. tropicalis* tadpoles and *E. coqui* embryos (with yolk removed) were anesthetized with neutral-buffered 2% MS-222, rinsed three times in PBS and snap frozen until extraction. On average, *E. coqui* embryos were more densely packed in T_3 solution (5.9 mg tissue per mL media) than *X. tropicalis* tadpoles (2.0 mg tissue per mL media); however, *E. coqui* embryos are routinely cultured in these conditions with no ill effects. Tissue was extracted as described above. Because we measured whole body content of stable isotope-labeled T_3 as a proxy for T_3 uptake, we used 25 ng of stable isotope-labeled rT_3 as an internal standard to correct for extraction efficiency.

Tissue Explant Culture and T_3 Treatments

To further investigate if thyroid axis components in the *E. coqui* limb and tail are functional, we cultured *E. coqui* and *X. tropicalis* limb and tail explants (30, 31), treated them with T_3, and assayed gene expression. We treated NF stage 52–54 (32) *X. tropicalis* tadpoles and TS stage 9 *E. coqui* embryos with 50 U/mL of penicillin-streptomycin added to aquarium or Petri dish solution for 24 h prior to dissection. Tadpoles and embryos were terminally anesthetized and dipped into 70% ethanol to sterilize the epidermis before dissection. Four *X. tropicalis* and two *E. coqui* individuals were pooled to make a single biological replicate of each species. Tissues were dissected into ice-cold 1:1.5-diluted Leibowitz-15 media (Gibco) containing 50 U/mL penicillin-streptomycin, 50 mg/mL gentamicin and 10 mM HEPES. Prior to T_3 treatment tissues were cultured overnight in media supplemented with insulin (500 ug/mL) on a laboratory bench at room temperature (21°C) with gentle shaking (50 rpm). The next morning, stock T_3 was diluted in 0.01 N NaOH and added to the media to a final concentration of 50 nM. Media and T_3 were changed every 8–12 h. After treatment for 8 or 46 h, limb and tail explants were rinsed three times in phosphate-buffered saline (PBS) and homogenized in TriZol. RNA was isolated according to the manufacturer's protocol.

Statistical Analysis

Statistical analyses of qPCR data were done with RStudio version 1.0.136 and visualized with ggplot2 (https://ggplot2.tidyverse.org/). Developmental timeline qPCR and iodothyronine content data followed a non-normal distribution as determined by Q-Q plots and the Shapiro-Wilk test; Levene's test determined that TH content data additionally had unequal variance. Log_{10}-transformed data were not normally distributed. Therefore, a Kruskal-Wallis test was used to determine if there were significant differences among groups, and a *post-hoc* Dunn's test with the Benjamini and Hochberg (BH) correction was used to identify stages that differ from each other while adjusting for multiple comparisons. We performed a least squares regression on T_4, T_3, and rT_3 data sets to investigate possible differences in iodothyronines kinetics during development. For the developmental timeline qPCR data, statistical tests were performed on data pooled from two independent experiments (see **Supplementary Data** for data from each experiment). For *in vivo* and *in vitro* T_3 treatment experiments, Student's *t*-test was used to identify significant differences between T_3-treated groups and controls.

RESULTS

Predicted Proteins of Isolated *E. coqui* cDNAs Contain Conserved Domains

Most isolated cDNAs contained functional domains of orthologous proteins. The predicted *E. coqui* TRα and TRβ sequences cover amino acids 11–281 (65%), and amino acids 9–273 (69%) of the orthologous *X. tropicalis* proteins, respectively. Both predicted TR protein sequences contain the DNA-binding domain and most of the ligand-binding domain. Alignments show that the predicted protein sequence of the *E. coqui* TRα DNA-binding domain has 97% identity to the *X. tropicalis* DNA-binding domain, while the TRα ligand-binding domain shared between the predicted *E. coqui* and *X. tropicalis* sequences

are 98% identical. The DNA-binding domain of the predicted *E. coqui* TRβ sequence is 100% identical to the DNA-binding domain in *X. tropicalis* TRβ, and the ligand-binding domain is 95% identical. The predicted partial *E. coqui* Dio2 sequence covers amino acids 2–254 (98%) of *X. tropicalis* Dio2 and the partial *E. coqui* Dio3 sequence covers amino acids 7–252 (90%) of *X. tropicalis* Dio3. Additionally, the predicted protein sequence of both *dio2* and *dio3* isolated cDNAs contain the selenocysteine site and the thioredoxin domain. Both thioredoxin domains share 86% identity with the orthologous *X. tropicalis* thioredoxin domain. The partial predicted amino acid sequence of *E. coqui Klf9* covers amino acids 194–264 (25%) of *X. tropicalis Klf9* and contains the three characteristic zinc-finger domains (100% identity) in the C-terminus of *X. tropicalis Klf9*. The isolated *E. coqui thibz* sequence covers amino acids 159–335 (53%) of *X. tropicalis* NFIL3-like (synonym for *thbzip*) and lacks the highly conserved basic leucine zipper domain. Even without the highly conserved basic leucine zipper domain, the predicted *E. coqui* protein sequence still clusters with other orthologous NFIL3-like proteins, rather than with other proteins with the basic leucine zipper domain (NFIL3 and CREB1) in maximum likelihood trees of these three orthologous vertebrate proteins (data not shown). Similarly, the other partial predicted *E. coqui* sequences cluster with other orthologous genes rather than with other closely related proteins containing similar domains (data not shown). We confirmed all isolated *E. coqui* cDNAs against the full-length transcript provided by investigators listed in the methods. Finally, we also performed BLASTx and BLASTn searches with the isolated *E. coqui* cDNA sequences. All cloned sequences have high similarity to predicted orthologous genes in frog species and other vertebrates (**Supplementary Table 4**).

Changes in Whole Body Iodothyronine Content During Embryonic *E. coqui* Development

Using LC-MS/MS, we detected the iodothyronines T_4, T_3, and rT_3 in unfertilized oocytes and at every stage of development (**Figure 2**). Thyroxine content (pg/mg body weight) was highest, followed by rT_3 and then T_3. We detected T_2 only at TS stages 14 and 15, when hatching occurs, and at this point, T_2 content was less than all other iodothyronine content and ranged between 0.04 and 0.78 pg/mg body weight (**Supplementary Table 3**). The three quantifiable iodothyronines were low and relatively constant up to TS stage 8, after which stage they showed statistically significant increases [T_3: Kruskal-Wallis rank sum test, $X^2 = 43.2$ (df = 15), $p < 0.001$; T_4: Kruskal-Wallis rank sum test, $X^2 = 43.7$ (df = 15), $p < 0.001$; rT_3: Kruskal-Wallis rank sum test, $X^2 = 39.7$ (df = 14), $p < 0.001$]. Whole body content of all three iodothyronines showed statistically significant increases between stages 8 and 13 (*post-hoc* Dunn's test; $p = 0.048$, 0.033, 0.035 for T_3, T_4, and rT_3, respectively). The velocity of change was slower for rT_3 and T_3 compared with T_4. Stage was a significant predictor for all three iodothyronines [T_3: $F = 70.8$ (df = 45), $p < 0.001$; T_4: $F = 54.2$ (df = 46) $p < 0.001$; rT_3: $F = 23.7$ (df = 43), $p < 0.001$]. Although all iodothyronines are positively correlated with stage, the velocity of change was slower for rT_3 and T_3 (slope of least squares regression (LSR) line, b = 0.2964 and 0.1009, respectively) compared to T_4 (LSR, b = 0.7984). Tissue content of all three iodothyronines was highest at TS 15. Note also that oocytes and early embryos (TS 0–5) of *E. coqui* have large yolk deposits, which may increase the S/N ratio and cause an underestimation of iodothyronine content in the embryo and yolk at these stages.

Changes in Thyroid Hormone Receptor and Deiodinase mRNA Levels in the Embryonic Tail

Both *thra* and *thrb* mRNAs in the *E. coqui* tail showed statistically significant changes during development [**Figure 3A**; *thra*: Kruskal-Wallis rank sum test, $X^2 = 20.18$ (df = 4), $p < 0.001$; *thrb*: Kruskal-Wallis rank sum test, $X^2 = 26.78$ (df = 4), $p < 0.001$]. *Thyroid hormone receptor α* and *thrb* mRNA in the tail bud are approximately equal at TS stage 5 (**Figure 3A**). *Thyroid hormone receptor α* mRNA in the tail at hatching is between 2.1- and 4-fold higher than the early tail (TS stages 5 and 7, *post-hoc* Dunn's test, $p = 0.002$ and 0.03, respectively). *Thyroid hormone receptor β* mRNA follows a similar pattern—it increased 4-fold between the onset of tail resorption (TS 13) and hatching (TS 15)—although *thra* increased only 1.8-fold over the same interval (**Figure 3A**). *Thyroid hormone receptor β* mRNA at hatching (TS 15) is between 18- and 47-fold higher than in the early tail (TS stage 5 and TS stage 7, *post-hoc* Dunn's test, $p < 0.001$ and $p = 0.002$, respectively).

Deiodinase type II and *dio3* mRNAs significantly changed during tail development (**Figure 3B**; *dio2*: Kruskal-Wallis rank sum test, $X^2 = 17.37$ (df = 4), $p = 0.002$; *dio3*: Kruskal-Wallis rank sum test, $X^2 = 26.11$ (df = 4), $p < 0.001$). Patterns of deiodinase mRNA in the developing tail were essentially the opposite of those seen in the limb. *Deiodinase type II* mRNA was low throughout tail development and resorption but rose almost 10-fold as hatching neared (TS 15; **Figure 3B**). At hatching (TS 15), *dio2* mRNA was higher than at TS 5, 7 and 13 (*post-hoc* Dunn's test, $p = 0.001$, 0.029, and 0.031, respectively). *Deiodinase type III* mRNA increased 27-fold between TS 5 and 13 (*post-hoc* Dunn's test, $p < 0.001$) and then decreased steeply (11-fold) between the onset of tail resorption and hatching (*post-hoc* Dunn's test, $p = 0.007$). Repeated experiments demonstrate the similar patterns of *thra*, *thrb*, *dio2*, and *dio3* expression (**Supplementary Figure 1**).

Changes in Thyroid Hormone Receptor and Deiodinase mRNA Levels in the Embryonic Hind Limb

Both *thra* and *thrb* mRNAs in the *E. coqui* hind limb showed statistically significant changes during development (**Figure 4A**; *thra*: Kruskal-Wallis rank sum test, $X^2 = 20.66$ (df = 4), $p < 0.001$; *thrb*: Kruskal-Wallis rank sum test, $X^2 = 25.36$ (df = 4), $p < 0.001$). The level of *thra* mRNA was greater than *thrb* mRNA in the limb bud until TS 10, when the *thra* mRNA level began to decrease and continued to decline through hatching (**Figure 4A**). The peak *thra* mRNA level at TS 10 coincides with the appearance of thyroid follicles (13); *thra* mRNA in the hind

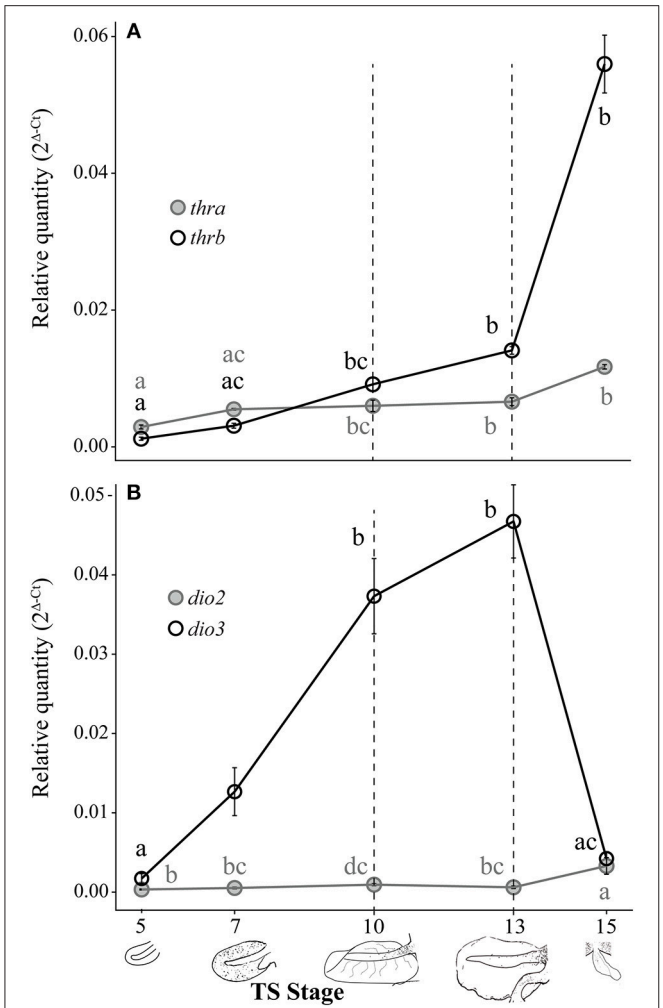

FIGURE 3 | Relative *thra* and *thrb* mRNA levels **(A)** and *dio2* and *dio3* mRNA levels **(B)** in the pre-hatching tail of *E. coqui*. Dashed vertical line at TS stage 10 marks when thyroid follicles are first visible in histological sections; the line at TS 13 indicates the onset of tail resorption. Drawings on the x-axis depict tail growth and resorption before hatching. Each expression value is represented as a circle centered on the mean of 3–7 individuals ± SE. Lower-case letters in gray (*thra* and *dio2*) and black (*thrb* and *dio3*) indicate significant pairwise differences between groups (*post-hoc* Dunn's test, $p < 0.05$). See **Supplementary Data** for a complete list of pairwise comparisons.

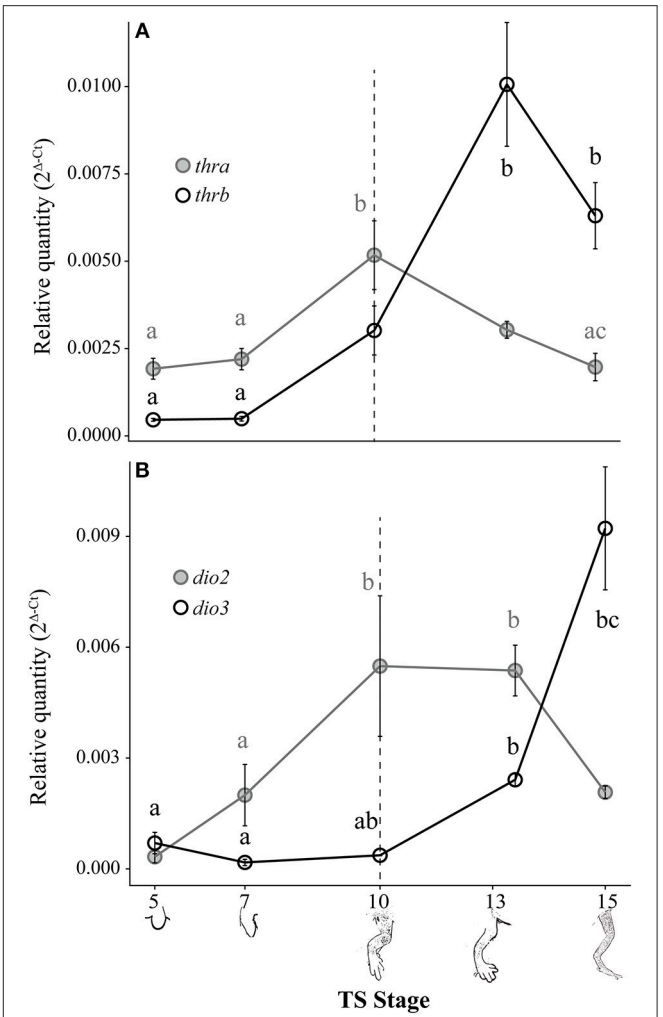

FIGURE 4 | Relative *thra* and *thrb* mRNA levels **(A)** and *dio2* and *dio3* mRNA levels **(B)** in the pre-hatching hind limb of *E. coqui*. Dashed vertical line at TS stage 10 marks when thyroid follicles are first visible in histological sections. Drawings on the x-axis depict sequential formation of the limb. Each expression value is represented as a circle centered on the mean of 5–7 hind limb pairs ± SE. Lower-case letters in gray (*thra* and *dio2*) and black (*thrb* and *dio3*) indicate significant pairwise differences between groups (*post-hoc* Dunn's test, $p < 0.05$). See **Supplementary Data** for a complete list of pairwise comparisons.

limb at this stage was significantly higher than in the limb bud at TS 5 (*post-hoc* Dunn's test, $p = 0.001$), in the limb paddle at TS stage 7 ($p = 0.009$) and in the fully formed froglet limb at TS 15 (*post-hoc* Dunn's test, $p = 0.002$). At hatching, *thra* mRNA level was lower than *thrb* mRNA levels. Between paddle (TS 7) and toepad formation (TS 13), *thrb* mRNA rose ∼21-fold to a peak at TS 13. At TS 13, *thrb* expression was significantly higher than in the limb bud and paddle (**Figure 4A**; TS 5 and 7; *post-hoc* Dunn's test, $p < 0.001$ and p = 0.001, respectively). *Thyroid hormone receptor β* mRNA drops almost 1.5-fold between TS 13 and hatching.

Deiodinase type II and *dio3* mRNAs both showed statistically significant but contrasting patterns throughout limb development [**Figure 4B**; *dio2*: Kruskal-Wallis rank sum test, $X^2 = 18.65$ (df = 4), $p < 0.001$; *dio3*: Kruskal-Wallis rank sum test, $X^2 = 25.76$ (df = 4), $p < 0.001$]. *Deiodinase type II* mRNA increased 16-fold between limb bud (TS 5) and digit formation (TS 10) and remained at this level through subsequent limb growth (TS 13; *post-hoc* Dunn's test, $p = 0.007$ and $p < 0.001$, respectively). *Deiodinase type II* mRNA decreased 2.6-fold between TS 13 and hatching to the level originally present in the newly formed limb bud (e.g., TS 5). *Deiodinase type III* mRNA remained low throughout most of limb development, but it increased 25-fold between the initial formation of thyroid follicles (TS 10) and hatching (TS 15; *post-hoc* Dunn's test, $p = 0.001$). Repeated experiments show the same general

contrasting mRNA expression patterns for *dio2*, *dio3*, *thra*, and *thrb* (**Supplementary Figure 2**).

Exogenous T_3 Induced Gene Expression Responses in the TS 9 *E. coqui* Tail, but Not the Limb

To determine if *E. coqui* tissues are capable of mounting a gene regulation response to exogenous T_3, we performed *in vivo* T_3 treatments (**Figure 5A**). Immersion of TS 9 *E. coqui* embryos in 50 nM T_3 for 8 h caused a significant induction of *klf9* (Student's *t*-test, $t = 5.61$ (df = 21.74), $p < 0.001$) and *thibz* (Student's *t*-test, $t = 6.20$ (df = 12.42), $p < 0.001$) in the tail. Immersion in 50 nM T_3 for 46 h additionally significantly induced *thrb* mRNA (**Supplementary Figure 4**). In contrast, the identical treatment significantly increased only *thibz* expression (**Figure 5B**; Student's *t*-test, $t = 3.11$ (df = 18.92), $p = 0.006$) in the limb.

E. coqui Embryos Took up Significantly Less T_3 From the Environment Than Did *X. tropicalis* Tadpoles

Because previous studies suggested that *E. coqui* limbs are insensitive to TH, and because we observed a weak TH response in our *in vivo* experiments, we wanted to confirm that immersion in T_3 increased tissue content of T_3. We quantified stable isotope-labeled T_3 tissue content after immersing *X. tropicalis* tadpoles or *E. coqui* embryos in stable isotope-labeled T_3 solution under three conditions. We chose 50 nM T_3 and 46 h treatment to match the *E. coqui in vivo* T_3 response experiments. We also chose two conditions that represent relevant time points from previous studies of larval *Xenopus* species: (1) treatment with 1 nM T_3 for 8 h is sufficient for *X. tropicalis*' whole body T_3 content to surpass the T_3 concentration in the surrounding media (33), and (2) treatment with 1 nM T_3 for 24 h is sufficient to induce gene expression responses in *X. tropicalis* (31, 34). After immersing *E. coqui* in 1 nM labeled T_3 for 8 and 24 h, we detected endogenous T_3 but not labeled T_3. However, we detected labeled T_3 in *X. tropicalis* tissue at both 8 and 24 h (**Table 2**). We detected stable isotope-labeled T_3 in both *E. coqui* and *X. tropicalis* tissue following 46-h treatment with 50 nM T_3. Total content of labeled T_3 in *X. tropicalis* tissue was ∼63 times that found in *E. coqui* tissues [**Table 2**, Student's *t*-test, $t = -3.20$ (df = 2.00), $p = 0.085$]. Additionally, *X. tropicalis* has ∼ 875 times more stable isotope-labeled T_3 than endogenous T_3 content. In contrast, stable isotope-labeled T_3 in *E. coqui* is approximately equal to endogenous T_3 content.

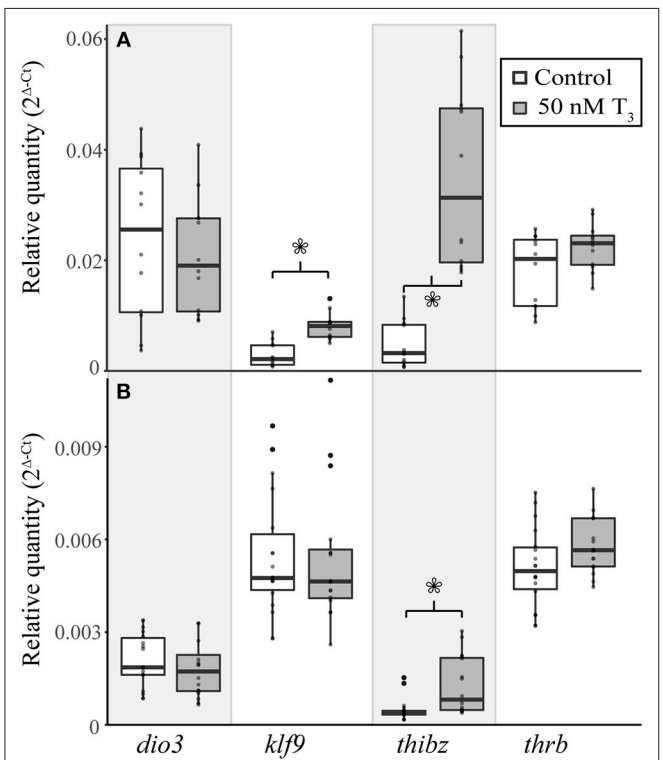

FIGURE 5 | Exogenous treatment with 50 nM T_3 for 8 h induces gene expression in the tail of *E. coqui* embryos at TS stage 9 **(A)**, but not in limbs at the same stage **(B)**. Boxes and whiskers depict the median and range of 12–16 individuals from two independent experiments. Asterisks indicate a significant change in expression (Student's *t*-test, $p < 0.05$).

Exogenous T_3 Strongly Induced T_3 Response Genes in TS Stage 9 *E. coqui* Limb Explants

Treatment with 50 nM T_3 for 8 h significantly increased *dio3* [Student's *t*-test, $t = 8.40$ (df = 4.00), $p = 0.001$), *klf9* (Student's *t*-test, $t = 14.41$ (df = 4.18), $p < 0.001$], *thibz* [Student's *t*-test, $t = 9.64$ (df = 4.01), $p < 0.001$], and *thrb* [Student's *t*-test, $t = 8.26$ (df = 4.39), $p < 0.001$] mRNAs in explants of *X. tropicalis* tail (**Figure 6A**). The same treatment caused a significant increase in *dio3* [Student's *t*-test, $t = 3.49$ (df = 3.00), $p = 0.040$], *klf9* [Student's *t*-test, $t = 13.66$ (df = 3.08), $p < 0.001$], and *thibz* [Student's *t*-test, $t = 21.50$ (df = 2.07), $p = 0.002$] mRNAs in *X. tropicalis* limb explants (**Figure 6B**). Similarly, exogenous T_3 increased *dio3* [Student's *t*-test, $t = 2.56$

TABLE 2 | Nieuwkoop and Faber stage 51–55 *Xenopus tropicalis* tadpoles have more labeled T_3 tissue content than do TS stage 9 *E. coqui* embryos after immersion in labeled T_3 for 8, 24, or 46 h.

Species	Labeled T_3 concentration (nM)	Timepoint (h)	Labeled T_3 pg/mg	T_3 pg/mg
X. tropicalis	1	8	1.079 ± 0.19	0.095 ± 0.02
E. coqui	1	8	0.000 ± 0.00	0.236 ± 0.01
X. tropicalis	1	24	1.371 ± 0.08	0.018 ± 0.01
E. coqui	1	24	0.000 ± 0.00	0.245 ± 0.04
X. tropicalis	50	46	30.436 ± 9.37	0.035 ± 0.01
E. coqui	50	46	0.483 ± 0.27	0.447 ± 0.20

Each value represents the mean of 3–6 individuals ± standard error.

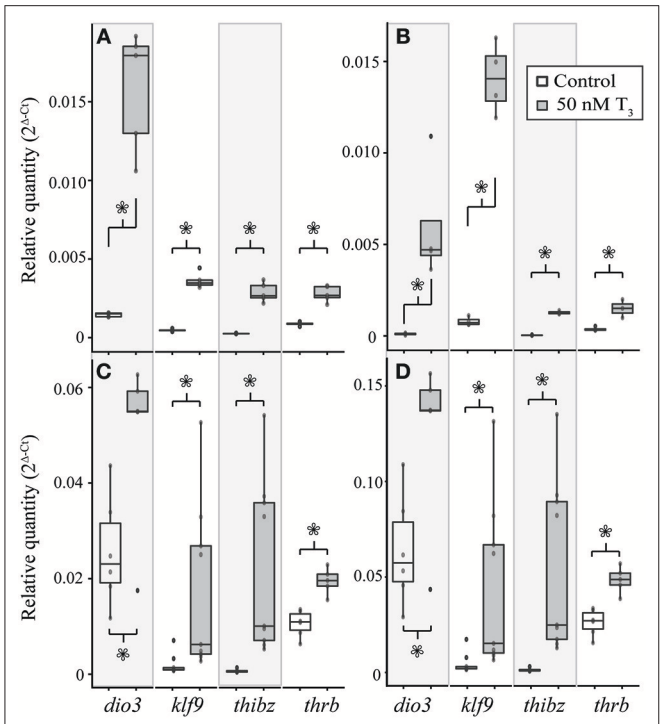

FIGURE 6 | Treatment with 50 nM exogenous T_3 for 8 h induces *deiodinase type III* (*dio3*), *krüppel-like factor 9* (*klf9*), *thyroid hormone induced bZip protein* (*thibz*), and *thrb* expression in NF stage 52–54 *X. tropicalis* tail **(A)** and limb **(B)** explants and in TS stage 9 *E. coqui* tail **(C)** and limb explants **(D)**. Asterisks indicate a significant increase in mRNA levels (Student's *t*-test, $p < 0.05$).

(df = 6.47), $p = 0.040$], *klf9* [Student's *t*-test, $t = 2.67$ (df = 8.22), $p = 0.028$], *thibz* [Student's *t*-test, $t = 3.54$ (df = 8.00), $p = 0.008$], and *thrb* [Student's *t*-test, $t = 5.38$ (df = 8.62), $p < 0.001$] mRNAs in explants of *E. coqui* tail (**Figure 6C**). *Deiodinase type III* [Student's *t*-test, $t = 2.61$ (df = 9.80), $p = 0.027$], *klf9* [Student's *t*-test, $t = 6.11$ (df = 8.05), $p < 0.001$], *thibz* [Student's *t*-test, $t = 6.49$ (df = 8.00), $p < 0.001$], and *thrb* [Student's *t*-test, $t = 7.70$ (df = 8.80), $p < 0.001$] increased after the same treatment in *E. coqui* limb explants (**Figure 6D**).

In both species, the magnitude of increase for all genes was greater in the limb than in the tail (**Table 3**). The same trends were observed after treating tissue explants with 50 nM T_3 for 46 h (**Supplementary Figure 5**). In tail explants, T_3 induced fold changes of a similar order of magnitude for *thibz* (between 42- and 44-fold) and *thrb* (between 1.8- and 3.8-fold), but not for *dio3* and *klf9*; in *E. coqui*, *dio3*, and *klf9* mRNAs increased 2- and 9.9-fold, respectively, while *dio3* and *klf9* mRNAs increased 11.9- and 12.5-fold in *X. tropicalis*. In limb explants, *dio3* and *thibz* mRNA differed by an order of magnitude between species. *Deiodinase type III* mRNA increased 58.8-fold in *X. tropicalis* limb explants, while *dio3* mRNA increased 3.7-fold in *E. coqui* limb tissue. *Thyroid hormone induced bZip protein* mRNA increased only 37-fold in *X. tropicalis* limb explants, while *dio3* mRNA increased 180-fold in *E. coqui* limb explants.

TABLE 3 | Induction of *deiodinase type III* (*dio3*), *krüppel-like factor 9* (*klf9*), *thyroid hormone induced bZip protein* (*thibz*), and *thyroid hormone receptor β* (*thrb*) in tail and limb explants of NF stages 52–54 *Xenopus tropicalis* and TS stage 9 *Eleutherodactylus coqui* after treatment with 50 nM T_3 for 8 h.

		Average fold increase	
Species	**Gene**	**Tail**	**Limb**
X. tropicalis	*dio3*	11.9	58.8
	klf9	12.5	17.8
	thibz	43.8	37.1
	thrb	3.8	4.0
E. coqui	*dio3*	2.0	3.7
	klf9	9.9	21.3
	thibz	42.0	180.0
	thrb	1.8	3.0

Values represent the average fold increase above control (vehicle-treated) levels.

DISCUSSION

In this study we show that the core TH signaling components are evolutionarily conserved in *Eleutherodactylus coqui* limb and tail tissue. We also show that developmental patterns of *thra*, *thrb*, *dio2,* and *dio3* mRNAs, and whole-body TH content in *E. coqui* closely match those reported during metamorphosis of *Xenopus* species. We also find maternal T_4, T_3, and rT_3 in unfertilized eggs and early embryos of *E. coqui*, which may mediate TR signaling prior to embryonic thyroid gland formation. This is the first published report of TH metabolites and maternally derived TH in a direct-developing frog. Additionally, we demonstrate that *E. coqui* tissues show robust gene expression responses to exogenous T_3 similar to those seen in metamorphosing species. *Eleutherodactylus coqui* embryos take up much less T_3 from the environment compared with *X. tropicalis*. This difference likely explains the relatively weak and variable gene expression responses seen *in vivo* in *E. coqui*, and was likely a significant confounding factor for previously published results.

Developmental Profiles of Whole Body Iodothyronine Content

Temporal dynamics of whole-body iodothyronine content in direct-developing *E. coqui* mirror those described for indirect-developing frogs, which retain the ancestral biphasic life history: *Scaphiopus hammondii* (28), *Rana catesbeiana* (35), *Bufo marinus* (36), *Bufo japonicus* (37), and *Xenopus laevis* (33). Anuran metamorphosis comprises three successive stages: premetamorphosis, when little to no TH is present; prometamorphosis, when TH concentrations slowly rise; and a rapid metamorphic climax characterized by a peak in TH concentrations. The temporal profile of TH content in embryonic *E. coqui* similarly defines three successive periods: (1) Low TH content characterizes the first half of development, prior to thyroid follicle formation (TS 1–8). (2) After thyroid follicles appear, TH content gradually rises until tail resorption began (TS 9–12). (3) TH content dramatically increases, with a peak in TH at or just prior to hatching (TS 13–15). In addition to amphibians,

many other vertebrates experience peak concentrations of TH at life history transitions—at hatching in precocial birds (38), at the larval-to-juvenile transition in several fish species (39–41), at ∼14 days post-partum in rats and mice (42, 43), and at birth in humans (44).

Thyroid hormones are present throughout early embryogenesis and the subsequent period of pre-hatching development in *E. coqui* (TS 1–9), beginning up to eight days before thyroid follicles can be detected histologically (13). These hormones are almost certainly maternal in origin. Similarly, T_4 and T_3 have been detected in yolk and gastrulating embryos of four other anuran species—*Bufo marinus* (36), *Rana catesbeiana* (35), *Bombina orientalis* (45), and *Xenopus laevis* (16). Early *Xenopus tropicalis* embryos express key TH signaling components (46). Indeed, TH signaling is also functional in the *Xenopus* tadpole central nervous system (CNS) before thyroid gland formation (16, 18). Maternally derived TH has a conserved role in vertebrate CNS development (47) and embryogenesis (17, 48, 49). Therefore, it seems likely that direct-developing frogs require maternal TH for normal neural development, as do most vertebrate species, although we do not evaluate that hypothesis here.

Maternal TH may regulate limb development occurring before the differentiation of the embryonic thyroid gland in direct-developing frogs. In metamorphosing anurans, TH signaling is required for terminal limb differentiation (22), but the initial stages of limb development are TH-independent. For example, tadpoles immersed in methimazole, a TH-synthesis inhibitor, develop a long limb-bud-like structure (24), and thyroidectomized tadpoles develop calcification centers in the hind limb (50, 51). In *E. coqui*, the limb bud proliferates and digits develop prior to the appearance of embryonic thyroid follicles (TS stages 9–10) [**Figure 3**; (8, 13)]. Two hypotheses could account for this observation: (1) *E. coqui* relies on maternal TH, rather than embryonically produced TH, to regulate early stages of digit patterning and growth (TS 6–9); or (2) paddle and digit formation in *E. coqui* proceed independently of TH. Our data show that requisite components of TH signaling are present at this time. Future investigation should evaluate the functional role of TH during this critical developmental period. A switch from embryonic to maternally synthesized TH for the regulation of early limb development, if it occurred, could explain the heterochronic shift in limb development and would represent an evolutionary novelty in direct-developing species.

Thyroid Hormone Receptor α, thrb, Dio2, and Dio3 mRNA Expression Patterns During Development and T3 Response in the Embryonic Tail

Tail resorption in *Xenopus tropicalis* occurs late in metamorphosis and is mediated by TRβ (52). Because tail resorption in *E. coqui* occurs late in embryogenesis and requires T_3 (8), we expected that *thra, thrb, dio2,* and *dio3* mRNA dynamics in the *E. coqui* tail would mirror those described in *Xenopus*. Our results support this hypothesis: in the *E. coqui* tail, a rise in *thrb* expression coincides with the rise in embryonic TH content, consistent with a role for *thrb* in mediating tail resorption.

Deiodinase type II and *dio3* mRNA expression patterns in the developing *E. coqui* tail are also similar to those described in indirect-developing species in which these deiodinase enzymes are critical for coordinating metamorphosis (20). Elevated *dio3* expression protects the tail from an early apoptotic response to T_3 until metamorphic climax in *Xenopus* (26); *E. coqui* tail resorption also begins at TS 13, when *dio3* expression significantly decreases. Although they serve different functions, the tail serves a critical role in both species: the larval *Xenopus* tail is a critical locomotor organ, whereas the embryonic *E. coqui* tail functions in respiration. In both species, maintenance of the tail is accomplished in part by *dio3* inactivation of T_4 and T_3.

Given the conservation of mRNA dynamics in the *E. coqui* tail, we wanted to determine whether the tissue could respond to exogenous T_3. In *Xenopus* species, treatment with exogenous T_3 induces transcription of direct T_3 response genes *dio3*, *klf9*, *thibz*, and *thrb* (19, 53–56). Exogenous T_3 induces significant increases in the mRNA of three of these T_3 response genes, *klf9*, *thibz*, and *thrb*, supporting the hypothesis that TH signaling components are conserved and mediate tail resorption in *E. coqui*.

Thyroid Hormone Receptor α, thrb, Dio2, and Dio3 mRNA Expression Patterns During Development and T_3 Response in the Embryonic Hind Limb

Thyroid hormone receptor α, thrb, dio2, and *dio3* mRNA expression patterns parallel those described in *Xenopus* species in the period leading up to and during metamorphosis (33, 57). In indirect-developing frogs, TRα has a critical role in controlling post-embryonic developmental timing (58–60) and in promoting proliferation in the hind limb during metamorphosis (61–63). Constitutive *thra* expression supports a proliferative and competence-establishing role for TRα in *E. coqui*. In the *E. coqui* limb, a rise in *thrb* expression coincides with the rise in embryonic TH content, consistent with TRβ autoinduction and tissue sensitization to TH described in *Xenopus* (64).

The tissue-specific patterns of *dio2* and *dio3* underlie the differential sensitivity of limb and tail tissue in metamorphosing frogs. *Deiodinase type II* expression is constitutive in the developing limb of *Xenopus laevis*, causing the limb to be sensitive to small amounts of T_3 produced during premetamorphosis (23). Similarly, elevated *dio2* expression in *E. coqui* limbs throughout most of limb development, including several days prior to formation of the embryonic thyroid gland, supports a role for TH-mediated limb development and growth.

In indirect-developing species, including *Xenopus* and spadefoot toads (*Scaphiopus*), concentrations between 1 and 10 nM T_3 are sufficient to promote precocious metamorphosis, tail resorption, and gene expression responses in limbs and tail (31, 65, 66). However, previous studies report that the

E. coqui limb has no morphological response to high doses of exogenous T_3 (11). Our study is the first to characterize mRNA expression changes in a direct-developing frog species in response to exogenous T_3. Treatment of *E. coqui* embryos with exogenous T_3 prior to formation of the thyroid follicles increases expression of four direct T_3 response genes in the tail, consistent with studies in *Xenopus* species (19, 53–55). However, limbs of the same embryos do not respond to T_3, despite the high dose administered (50 nM T_3). The lack of response previously observed in direct-developing species may be confounded by an inability of T_3 to reach the limb tissue. We observe a weak induction of T_3 response genes in TS stage 7 limbs, a full two days before *E. coqui* begins to produce TH (**Supplementary Figure 3**). It is possible that this response occurs because the adult epidermis is not yet fully formed and T_3 is better able to penetrate into the tissue, or because there is less endogenous T_3 present at TS 7 than at TS 9. In either case, the ability to respond to T_3 prior to thyroid gland formation is similar to biphasic species; tadpoles are also TH competent as soon as they hatch. Finally, the similar robust gene regulation response induced in *E. coqui* and *X. tropicalis* limb explants suggests that the limb tissue itself is similarly competent in both species. Overall, these data support the hypothesis that TH plays a role in *E. coqui* limb development and may do so prior to formation of the embryonic thyroid gland.

Here we support previous claims that later stages of limb development in *E. coqui* are TH-dependent but we additionally show that TH-signaling components are present during earlier stages, and that *E. coqui* limb tissue is sensitive to T_3. *Eleutherodactylus coqui* eggs are provisioned with maternally derived TH, which may mediate organogenesis before differentiation and activity of the embryo's own thyroid gland. Altogether, our data suggest that the TH-mediated molecular module active during post-hatching metamorphosis in indirect-developing frogs has been shifted prior to hatching in direct-developing species.

ETHICS STATEMENT

This study was carried out in accordance with the recommendations of the Harvard Faculty of Arts and Sciences Institutional Animal Care and Use Committee. The protocol was approved by the Harvard Faculty of Arts and Sciences Institutional Animal Care and Use Committee.

AUTHOR CONTRIBUTIONS

ML designed experiments and performed experiments, interpreted data, and wrote the manuscript. RD and JH contributed to experimental design, edited the manuscript, and discussed data interpretation.

FUNDING

This study was supported by a Graduate Women in Science Fellowship and NSF grant IOS 11456115 to RD, an NSF Doctoral Dissertation Improvement Grant #1701591, and Miyata and Goelet Grants from the Museum of Comparative Zoology. Published by a grant from the Wetmore Colles fund of the Museum of Comparative Zoology.

ACKNOWLEDGMENTS

We thank Laurent Sachs, Nicolas Buisine, Gwenneg Kerdivel, Austin Mudd, Richard Harland, and Dan Rokhsar for providing sequences that made this work possible. We also thank Charles Vidoudez for technical help in tissue extraction and TH quantification.

SUPPLEMENTARY MATERIAL

The Supplementary Material for this article can be found online at: https://www.frontiersin.org/articles/10.3389/fendo.2019.00307/full#supplementary-material

REFERENCES

1. Pough FH, Andrews R, Crump M, Savitzky AH, Wells KD, Brandley MC. *Herpetology*. 4th ed. Sunderland, MA: Sinauer Associates, Inc. (2015).
2. Elinson RP, del Pino EM. Developmental diversity of amphibians. *WIREs Dev Biol.* (2012) 1:345–69. doi: 10.1002/wdev.23
3. Hanken J, Klymkowsky MW, Summers CH, Seufert DW, Ingebrigsten N. Cranial ontogeny in the direct-developing frog, *Eleutherodactylus coqui* (Anura: Leptodactylidae), analyzed using whole-mount immunohistochemistry. *J Morphol.* (1992) 211:95–118. doi: 10.1002/jmor.1052110111
4. Denver RJ. Neuroendocrinology of amphibian metamorphosis. In: Shi Y-B, editor. *Current Topics in Developmental Biology*. Burlington: Elsevier Inc. (2013), 195–227.
5. Lynn WG. A Study of the Thyroid in Embryos of *Eleutherodactylus nubicola*. The Anatomical Record, 64, p.525-535, 2 plates.
6. Lynn WG, Peadon AM. The role of the thyroid gland in direct development in the Anuran, *Eleutherodactylus martinicensis*. *Growth.* (1955) 19:263–86.
7. Schlosser G, Roth G. Development of the retina is altered in the directly developing frog *Eleutherodactylus coqui* (Leptodactylidae). *Neurosci Lett.* (1997) 224:153–6. doi: 10.1016/S0304-3940(97)00174-2
8. Callery EM, Elinson RP. Thyroid hormone-dependent metamorphosis in a direct developing frog. *Proc Natl Acad Sci USA.* (2000) 97:2615–20. doi: 10.1073/pnas.050501097
9. Elinson RP. Metamorphosis in a frog that does not have a tadpole. In: Shi Y-B, editor. *Current Topics in Developmental Biology*. Vol. 103. Burlington: Elsevier Inc. (2013), 259–76. doi: 10.1016/B978-0-12-385979-2.00009-5
10. Lynn WG. The effects of thiourea and phenylthiourea upon the development of *Eleutherodactylus ricordii*. *Biol Bull.* (1948) 94:1–15. doi: 10.2307/1538202
11. Elinson RP. Leg development in a frog without a tadpole (*Eleutherodactylus coqui*). *J Exp Zool.* (1994) 270:202–10. doi: 10.1002/jez.1402700209
12. Townsend D, Stewart M. Direct development in *Eleutherodactylus coqui* (Anura: Leptodactylidae): a staging table. *Copeia.* (1985) 1985:423–36. doi: 10.2307/1444854
13. Jennings DH, Hanken J. Mechanistic basis of life history evolution in anuran amphibians: thyroid gland development in the direct-developing frog, *Eleutherodactylus coqui*. *Gen Comp Endocrinol.* (1998) 111:225–32. doi: 10.1006/gcen.1998.7111

14. Rosenkilde P. Thyroid hormone synthesis in metamorphosing and adult *Xenopus laevis*. *Gen Comp Endocrinol.* (1978) 34:95–6.
15. Buscaglia M, Leloup J, De Luze A. The role and regulation of monodeiodination of thyroxine to 3,5,3'-triidothyronine during amphibian metamorphosis. In: Balles M, Bownes M, editors. *Metamorphosis*. Oxford: Clarendon Press. (1985), 273–293.
16. Fini JB, Le Mével S, Palmier K, Darras VM, Punzon I, Richardson SJ, et al. Thyroid hormone signaling in the *Xenopus laevis* embryo is functional and susceptible to endocrine disruption. *Endocrinology.* (2012) 153:5068–81. doi: 10.1210/en.2012-1463
17. Morvan-Dubois G, Fini JB, Demeneix B. A. Is thyroid hormone signaling relevant for vertebrate embryogenesis? In: Shi Y-B, editor. *Current Topics in Developmental Biology*. Vol 103. Burlington: Elsevier Inc (2013), 365–96. doi: 10.1016/B978-0-12-385979-2.00013-7
18. Le Blay K, Préau L, Morvan-Dubois G, Demeneix B. Expression of the inactivating deiodinase, Deiodinase 3, in the pre-metamorphic tadpole retina. *PLoS ONE.* (2018) 13:e0195374. doi: 10.1371/journal.pone.0195374
19. Wang Z, Brown DD. Thyroid hormone-induced gene expression program for amphibian tail resorption. *J Biol Chem.* (1993) 268:16270–8.
20. Becker K, Stephens K. The type 2 and type 3 iodothyronine deiodinases play important roles in coordinating development in *Rana catesbeiana* tadpoles. *Endocrinology.* (1997) 138:2989–97. doi: 10.1210/endo.138.7.5272
21. Galton VA. Iodothyronine 5′-deiodinase activity in the amphibian *Rana catesbeiana* at different stages of the life cycle. *Endocrinology.* (1988) 122:1746–50.
22. Schreiber AM, Das B, Huang H, Marsh-Armstrong N, Brown DD. Diverse developmental programs of Xenopus laevis metamorphosis are inhibited by a dominant negative thyroid hormone receptor. *Proc Natl Acad Sci USA.* (2001) 98:10739–44. doi: 10.1073/pnas.191361698
23. Cai L, Brown DD. Expression of type II iodothyronine deiodinase marks the time that a tissue responds to thyroid hormone-induced metamorphosis in *Xenopus laevis*. *Dev Biol.* (2004) 266:87–95. doi: 10.1016/j.ydbio.2003.10.005
24. Brown DD, Cai L, Das B, Marsh-Armstrong N, Schreiber A, Juste R. Thyroid hormone controls multiple independent programs required for limb development in *Xenopus laevis* metamorphosis. *Proc Natl Acad Sci USA*. (2005) 102:12455–8. doi: 10.1073/pnas.0505989102
25. Buchholz DR, Paul BD, Fu L, Shi Y-B. Molecular and developmental analyses of thyroid hormone receptor function in *Xenopus laevis*, the African clawed frog. *Gen Comp Endocrinol.* (2006) 145:1–19. doi: 10.1016/j.ygcen.2005.07.009
26. Nakajima K, Fujimoto K, Yaoita Y. Regulation of thyroid hormone sensitivity by differential expression of the thyroid hormone receptor during *Xenopus* metamorphosis. *Genes Cells.* (2012) 17:645–59. doi: 10.1111/j.1365-2443.2012.01614.x
27. Denver RJ. Acceleration of anuran amphibian metamorphosis by corticotropin-releasing hormone-like peptides. *Gen Comp Endocrinol.* (1993) 91:38–51. doi: 10.1006/gcen.1993.1102
28. Denver RJ. Hormonal correlates of environmentally induced metamorphosis in the western spadefoot toad, *Scaphiopus hammondii*. *Gen Comp Endocrinol.* (1998) 110:326–36. doi: 10.1006/gcen.1998.7082
29. Schmittgen TD, Livak KJ. Analyzing real-time PCR data by the comparative CT method. *Nat Protoc.* (2008) 3:1101–8. doi: 10.1038/nprot.2008.73
30. Tata JR, Kawahara A, Baker BS. Prolactin inhibits both thyroid hormone-induced morphogenesis and cell death in cultured amphibian larval tissues. *Dev Biol.* (1991) 146:72–80. doi: 10.1016/0012-1606(91)90447-B
31. Bonett RM, Hoopfer ED, Denver RJ. Molecular mechanisms of corticosteroid synergy with thyroid hormone during tadpole metamorphosis. *Gen Comp Endocrinol.* (2010) 168:209–19. doi: 10.1016/j.ygcen.2010.03.014
32. Nieuwkoop P, Faber J. *Normal Table of Xenopus laevis (Daudin)*. New York, NY: Garland Publishing Inc. (1994). Available online at: http://www.xenbase.org/anatomy/alldev.do.
33. Krain LP, Denver RJ. Developmental expression and hormonal regulation of glucocorticoid and thyroid hormone receptors during metamorphosis in *Xenopus laevis*. *J Endocrinol.* (2004) 181:91–104. doi: 10.1677/joe.0.1810091
34. Bagamasbad PD, Bonett RM, Sachs L, Buisine N, Raj S, Knoedler JR, et al. Deciphering the regulatory logic of an ancient, ultraconserved nuclear receptor enhancer module. *Molecul Endocrinol.* (2015) 29:856–72. doi: 10.1210/me.2014-1349
35. Fujikara K, Suzuki S. Thyroxine and thyroglobulin in eggs and embryos of bullfrog. *Zool Sci.* (1991) 8:1166.
36. Weber GM, Farrar ES, Tom CKF, Grau EG. Changes in whole-body thyroxine and triiodothyronine concentrations and total content during early development and metamorphosis of the toad *Bufo marinus*. *Gen Comp Endocrinol.* (1994) 94:62–71. doi: 10.1006/gcen.1994.1060
37. Niinuma TM, Hirano T, Kikuyama S. Changes in tissue concentrations of thyroid hormones in metamorphosing toad larvae. *Zool Sci.* (1991) 8:345–50.
38. De Groef B, Grommen SVH, Darras VM. Hatching the cleidoic egg: the role of thyroid hormones. *Front Endocrinol.* (2013) 4:1–10. doi: 10.3389/fendo.2013.00063
39. Brown D. The role of thyroid hormone in zebrafish and axolotl development. *Proc Natl Acad Sci USA*. (1997) 94:13011–6. doi: 10.1073/pnas.94.24.13011
40. De Jesus EGT, Toledo JD, Simpas MS. Thyroid hormones promote early metamorphosis in grouper (*Epinephelus coioides*) larvae. *Gen Comp Endocrinol.* (1998) 112:10–6. doi: 10.1006/gcen.1998.7103
41. Reddy PK, Lam TJ. Role of thyroid hormones in tilapia larvae (*Oreochromis mossambicus*): 1. *Effects of the hormones and an antithyroid drug on yolk absorption, growth and development*. *Fish Physiol Biochem.* (1992) 9:473–85. doi: 10.1007/BF02274228
42. Babu S, Sinha RA, Mohan V, Rao G, Pal A, Pathak A, et al. Effect of hypothyroxinemia on thyroid hormone responsiveness and action during rat postnatal neocortical development. *Exp Neurol.* (2011) 228:91–8. doi: 10.1016/j.expneurol.2010.12.012
43. Hadj-Sahraoui N, Seugnet I, Ghorbel MT, Demeneix B. Hypothyroidism prolongs mitotic activity in the post-natal mouse brain. *Neurosci Lett.* (2000) 280:79–82. doi: 10.1016/S0304-3940(00)00768-0
44. Buchholz DR. More similar than you think: Frog metamorphosis as a model of human perinatal endocrinology. *Dev Biol.* (2015) 408:188–95. doi: 10.1016/j.ydbio.2015.02.018
45. Jennings, D. H. (1997). *Evolution of Endocrine Control of Development in Direct-Developing Amphibians*. Unpublished Ph.D. dissertation. University of Colorado, Boulder.
46. Duarte-Guterman P, Langlois VS, Pauli BD, Trudeau VL. Expression and T3 regulation of thyroid hormone- and sex steroid-related genes during *Silurana (Xenopus) tropicalis* early development. *Gen Comp Endocrinol.* (2010) 166:429–35. doi: 10.1016/j.ygcen.2009.12.008
47. Bernal J. Thyroid hormone receptors in brain development and function. *Nat Clin Pract Endocrinol Metab.* (2007) 3:249–59. doi: 10.1038/ncpendmet0424
48. Havis E, Le Mével S, Morvan Dubois G, Shi D, Scanlan TS, Demeneix B, et al. Unliganded thyroid hormone receptor is essential for *Xenopus laevis* eye development. *EMBO J.* (2006) 25:4943–51. doi: 10.1038/sj.emboj.7601356
49. Morvan Dubois G, Sebillot A, Kuiper GJM, Verhoelst CHJ, Darras VM, Visser TH, et al. Deiodinase activity is present in *Xenopus laevis* during early embryogenesis. *Endocrinology.* (2006) 147:4941–9. doi: 10.1210/en.2006-0609
50. Terry GS. Effects of the extirpation of the thyroid gland upon ossification in *Rana pipiens*. *J Exp Zool.* (1918) 24:567–87. doi: 10.1002/jez.1400240306
51. Allen BM. The results of thyroid removal in the larvae of *Rana pipiens*. *J Exp Zool.* (1983) 24:499–519. doi: 10.1002/jez.1400240303
52. Nakajima K, Tazawa I, Yaoita Y. Thyroid hormone receptor α - and β - knockout *Xenopus tropicalis* tadpoles reveal subtype-specific roles during development. *Endocrinology.* (2017) 159:733–43. doi: 10.1210/en.2017-00601
53. Ranjan M, Wong J, Shi YB. Transcriptional repression of *Xenopus* TRβ gene is mediated by a thyroid hormone response element located near the start site. *J Biol Chem.* (1994) 269:24699–705.
54. Furlow DJ, Kanamori A. The transcription factor basic transcription element-binding protein 1 is a direct thyroid hormone response gene in the frog *Xenopus laevis*. *Endocrinology.* (2002) 143:3295–305. doi: 10.1210/en.2002-220126
55. Das B, Heimeier RA, Buchholz DR, Shi Y-B. Identification of direct thyroid hormone response genes reveals the earliest gene regulation programs during frog metamorphosis. *J Biol Chem.* (2009) 284:34167–78. doi: 10.1074/jbc.M109.066084
56. Helbing CC, Werry K, Crump D, Domanski D, Veldhoen N, Bailey CM. Expression profiles of novel thyroid hormone-responsive genes and proteins in the tail of *Xenopus laevis* tadpoles undergoing precocious metamorphosis. *Molecul Endocrinol.* (2003) 17:1395–409. doi: 10.1210/me.2002-0274

57. Yaoita Y, Brown DD. A correlation of thyroid hormone receptor gene expression with amphibian metamorphosis. *Genes Dev.* (1990) 4:1917–24. doi: 10.1101/gad.4.11.1917
58. Wen L, Shi YB. Unliganded thyroid hormone receptor α controls developmental timing in *Xenopus tropicalis*. *Endocrinology.* (2015) 156:721–34. doi: 10.1210/en.2014-1439
59. Choi J, Suzuki KT, Sakuma T, Shewade L, Yamamoto T, Buchholz D. Unliganded thyroid hormone receptor α regulates developmental timing via gene repression in *Xenopus tropicalis*. *Endocrinology.* (2015) 156:735–44. doi: 10.1210/en.2014-1554
60. Buchholz DR, Shi Y. Dual function model revised by thyroid hormone receptor alpha knockout frogs. *Gen Comp Endocrinol.* (2018) 265:214–8. doi: 10.1016/j.ygcen.2018.04.020
61. Denver RJ. The molecular basis of thyroid hormone-dependent central nervous system remodeling during amphibian metamorphosis. *Compar Biochem Physiol Part C, Pharmacol Toxicol Endocrinol.* (1998) 119:219–28. doi: 10.1016/S0742-8413(98)00011-5
62. Denver RJ, Hu F, Scanlan TS, Furlow DJ. Thyroid hormone receptor subtype specificity for hormone-dependent neurogenesis in *Xenopus laevis*. *Dev Biol.* (2009) 326:155–68. doi: 10.1016/j.ydbio.2008.11.005
63. Choi J, Ishizuya-Oka A, Buchholz DR. Growth, development, and intestinal remodeling occurs in the absence of thyroid hormone receptor a in tadpoles of *Xenopus tropicalis*. *Endocrinology.* (2017) 158:1623–33. doi: 10.1210/en.2016-1955
64. Tata JR. Autoinduction of nuclear hormone receptors during metamorphosis and its significance. *Insect Biochem Mol Biol.* (2000) 30:645–51. doi: 10.1016/S0965-1748(00)00035-7
65. Buckbinder L, Brown DD. Thyroid hormone-induced gene expression changes in the developing frog limb. *J Biol Chem.* (1992) 267:25786–91.
66. Buchholz DR, Hayes TB. Variation in thyroid hormone action and tissue content underlies species differences in the timing of metamorphosis in desert frogs. *Evol Dev.* (2005) 7:458–67. doi: 10.1111/j.1525-142X.2005.05049.x

Conflict of Interest Statement: The authors declare that the research was conducted in the absence of any commercial or financial relationships that could be construed as a potential conflict of interest.